Sun-synchronous spacecraft compliance with international space debris guidelines

Schild, Maarten; Noomen, Ron

DOI
10.1016/j.asr.2022.07.011

Publication date
2022

Document Version
Final published version

Published in
Advances in Space Research

Available online at www.sciencedirect.com

ScienceDirect

Advances in Space Research 72 (2023) 2585–2596

ADVANCES IN SPACE RESEARCH (a COSPAR publication)

www.elsevier.com/locate/asr

Sun-synchronous spacecraft compliance with international space debris guidelines

Maarten Schild *, Ron Noomen

Faculty of Aerospace Engineering, Delft University of Technology, Delft 2629HS, the Netherlands

Received 22 December 2021; received in revised form 25 June 2022; accepted 5 July 2022
Available online 15 July 2022

Abstract

Due to ever increasing accessibility, recent years have seen a fast growing number of launches to space, especially to Sun-synchronous orbit. The spent rocket parts, and eventually non-functioning payloads of these launches remain in orbit. It is well established that this accumulation of space debris over time is quickly making this the most severe threat to future spaceflight operations. To address this, international guidelines have been established including a maximum of 25-year remaining orbital lifetime after end of operational life. This paper evaluates if Sun-synchronous satellites adhere to this guideline. To determine the compliance, the operational status of satellites with orbital control capabilities is established using a maneuver detection algorithm. For satellites without this capability, a model is created based on mass and design lifetime. The remaining orbital lifetime is determined using semi-analytic propagation. The results reveal that compliance was poor in the past, with 20 to 40% prior to 2014, but has increased to 95% in 2018. Satellites with a mass lower than 10 kg have a compliance of 86% compared to 35% for heavier satellites. Analysis shows that compliance is mostly a result of choosing an operational orbit with a sufficient natural decay, and less due to altitude lowering maneuvers near end-of-life. The relative popularity of SSO may demand re-evaluation of current guidelines to sustain future operations in these valuable orbits.

Keywords: Space debris; Compliance; Sun-synchronous orbit; Maneuver detection; Semi-analytical propagation

1. Introduction

The spent rocket parts and eventually non-functioning payloads of spacecraft launches often remain in orbit around Earth. The accumulation of this space debris over time and the ever increasing accessibility to space is quickly making this the most severe threat to future spaceflight operations. Being uncontrollable, these space debris parts are creating collision risks with operational satellites and other space debris. Such a collision would result in new debris objects thereby increasing the likelihood of even more collisions, a cascading effect known as the Kessler syndrome, which could ultimately lead to entire orbits rendered completely unusable (Kessler and Cour-Palais, 1978).

As early as 1974 concerns were raised regarding the impact of this debris on spaceflight in the future (Brooks et al., 1974). Since then a large amount of research was done on this subject and recommendations and guidelines were established by multiple bodies, agencies and research groups to remedy this problem. As of writing there are four major guidelines in effect internationally: The European Code of Conduct for Space Debris Mitigation (Anselmo et al., 2004) established in 2004, the Inter-Agency Space Debris Coordination Committee Guidelines (IADC, 2002), first issued in 2002 with a revision in 2007, and the Committee on the Peaceful Uses of Outer Space (COPUOS) guidelines published in 2007. Furthermore, whereas the previously mentioned guidelines mainly

* Corresponding author.
E-mail address: maartenschild@gmail.com (M. Schild).

https://doi.org/10.1016/j.asr.2022.07.011
0273-1177/

involve governments and national space agencies, the International Organization for Standardization (ISO) aims to promote space debris mitigation and prevention design in the global space industry (Kato et al., 2013). Formally first issued in 2010, this top-level standard ISO 24113 involves multiple lower-level standards applicable to space debris mitigation. For a more in-depth history the reader is referred to the works of Bonnal (2016, 2019) and Johnson (2007).

Overall a strong international consensus on the importance and urgency of space debris regulations can be seen. Most of the guidelines however are not very directly worded. In this way it leaves room for interpretation and no clearly defined points where compliance can be determined; the major exception being the 25-year lifetime rule. This protects the low Earth orbit (LEO) region by limiting the time in orbit, after end-of-life, to 25 years.

The objective of this paper is to investigate the state of the space environment in Sun-synchronous orbit (SSO) and to determine if satellite operators adhere to this 25-year time limit after end-of-life. This will be done by first showing in Section 2 why SSO is such an important regime in the space debris problem. Following this, the methodology to determine compliance will be discussed in Section 3. Use is made of a maneuver detection algorithm and a design lifetime study, to be able to determine the operational status for satellites both with and without orbital control capabilities. Both are discussed in Section 4. The second major part is the orbital lifetime estimation which can be found in Section 5. These parts are combined to determine the compliance in Section 6. Finally, conclusions regarding the aforementioned aspects of the study and their outcomes, as well as recommendations on improvements and future studies will be given in Section 7.

2. Inventory of satellites

The majority of payloads in space are within LEO. Within this region they are not uniformly distributed but clearly clustered as shown in Fig. 1.

A large part of the objects in LEO are in SSO with an inclination of about 98°. In this study SSO is defined as having an inclination between 96.5 and 102.5 degrees and a perigee altitude of less than 2000 km. Other visible bands can be attributed to the Cosmos-3 M and Vostok stages and the Parus and Meteor satellites for $i \approx 82°$, and the International Space Station at $i \approx 52°$(de Luca et al., 2013). Note the log scale and thus high popularity of these specific inclination bands. Clearly visible as well are the bands corresponding to the Baikonur Cosmodrome at 45.6°, Guiana Space Centre at 5.2°, Kennedy Space Center at 28.6° and the Molniya satellites at 63°.

As can be seen more clearly in Fig. 2, the objects in SSO represent a large fraction of the total number of objects in LEO.

SSO has seen an enormous increase in launches from 2017 onwards, as shown, grouped by mass, in Fig. 3.

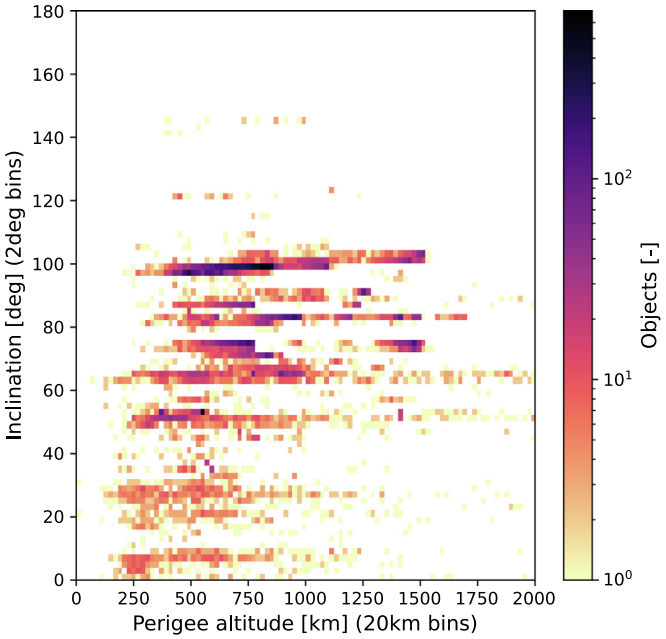

Fig. 1. Object distribution within LEO on January 1, 2021. Based on available TLE data provided by Space-Track (2021) at https://www.s.pace-track.org/.

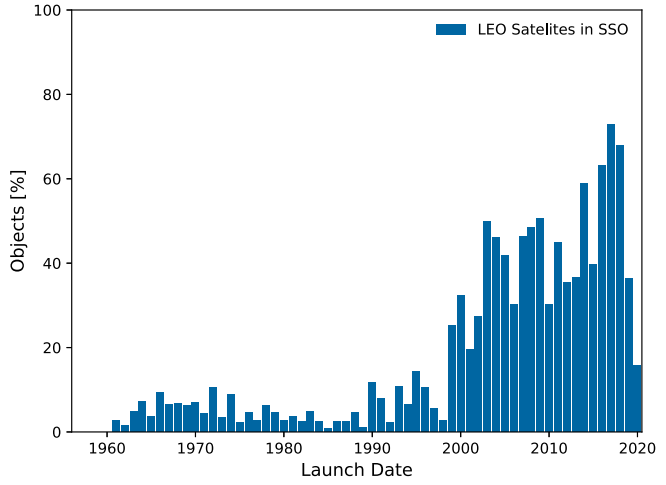

Fig. 2. Percentage of LEO satellites in SSO. Based on available TLE data provided by Space-Track (2021) at https://www.s.pace-track.org/.

During the past four years combined, as many objects have been launched as in all earlier years together (812 versus 817).

These increasing numbers are primarily driven by the very large increase of small satellites with a mass of less than 10 kg, made possible by modern technological miniaturization advancements. This popularity can be explained by the many advantages these orbits provide. First of all, due to the nature of the orbit, satellites pass over a particular part of the Earth with the same lighting conditions. These time-constant conditions are of benefit for many research and observation missions. This is combined with a relative low altitude providing excellent ground

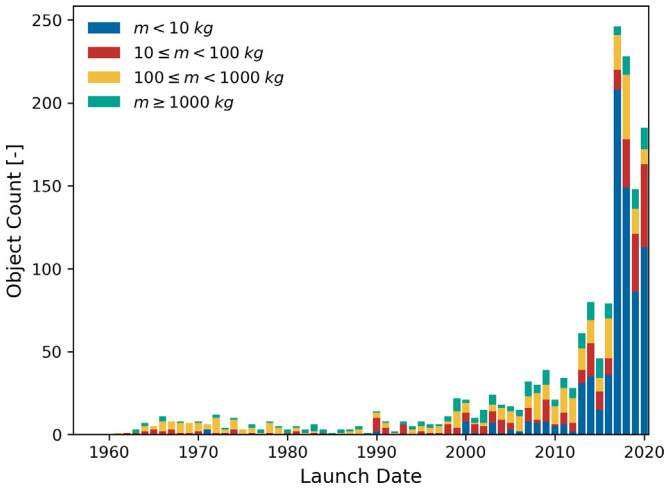

Fig. 3. Payload launch traffic into SSO over time for different mass categories. Based on available mass and launch date data provided by ESA (2021) at https://discoswe.b.esoc.esa.int/.

resolution and high inclination providing almost global coverage. The combination of its relative popularity and the advantages these orbits provide demand SSO's to be looked at in-depth, separate from the entire LEO regime. Strictly speaking, when a satellite (compliant or not) drops to a lower altitude, it will no longer satisfy the SSO conditions on the precession of the ascending node exactly. Still, the altitude and inclination will remain such that regular (twice per revolution) crossings with the orbits of real SSO spacecraft can be expected. Therefore it remains a potential threat to such satellites, and in principle the full duration of the lifetime needs to be taken into account for risk analyses. The orbital parameters of any satellite while operational are taken as the criterion to consider them as Sun-synchronous satellite or not.

3. Methodology

The method used to determine the compliance rate of Sun-synchronous satellites with the 25-year lifetime guideline can be split up in two main segments. As this 25-year lifetime countdown only starts after the operational phase is ended, first the operational status of the satellite needs to be determined. Afterwards, the remaining orbital lifetime in the protected region needs to be predicted. These can then be combined to determine the compliance of the satellite. This is done for the entire population of Sun-synchronous satellites to determine the overall compliance rate.

The determination of the operational status of a satellite is crucial to assess its compliance with the space debris mitigation guidelines. Most companies and institutions do publish extensively on their satellite launches. Unfortunately, they do not report it when a spacecraft is put out of service, or stops functioning because of a technical problem. There is also not a regulated central registry to look up this information. Therefore it was decided instead to use the long-term orbital behaviour of a spacecraft for reliable, unbiased classification.

For satellites with orbital control capabilities, first a long-term data set of the orbital parameters was obtained from Space-Track (2021). This data then has to be filtered to determine non-natural behaviour which would correspond to active control and therefore an active and operational satellite. How this was done will be shown in Section 4.1. If after a few years such a satellite would stop showing this active behaviour it can be assumed that the satellite has stopped functioning. For satellites without orbital control capabilities, such as many of the smaller satellites, this will of course not work. These two groups were therefore treated separately.

Using the methods described it can be determined if and when a satellite has become non-operational. From that point, as stated in the space debris guidelines, a satellite has a maximum of 25 years to leave the protected region. This can be done by a direct re-entry, but the most commonly chosen method is using natural orbital decay. Sometimes a small maneuver is also performed to lower the orbit to hasten this process.

By combining the information from the operational status determination using maneuver detection with the decay date obtained from the orbital lifetime prediction, the compliance of the satellite can finally be determined. The resulting algorithm is shown in the flowchart in Fig. 4.

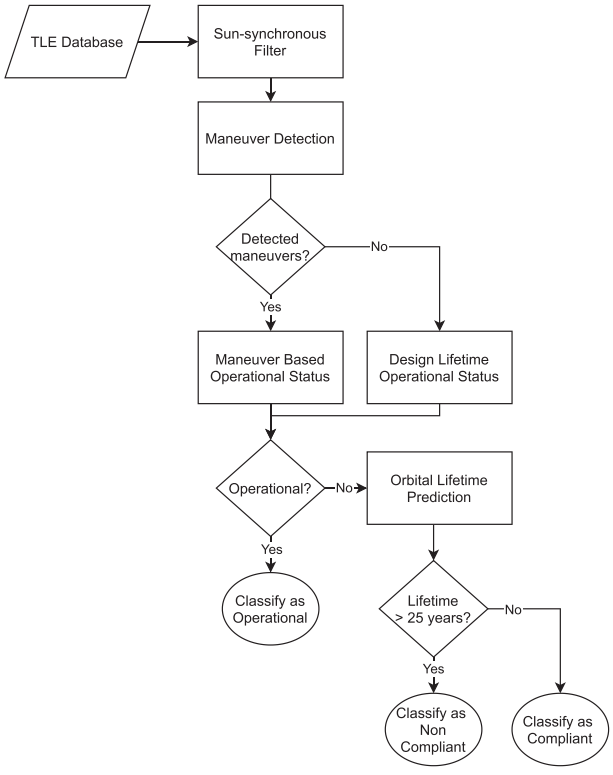

Fig. 4. Flowchart of the compliance rate determination algorithm.

The entire TLE database is first filtered for all satellites in a Sun-synchronous orbit. For each satellite it is determined when the last orbital maneuver was made in order to determine the operational status. A satellite is classified as active when it has made a maneuver within the past two years, but setting a different time limit would not change the outcome significantly.

If it has done maneuvers in the past but it stopped doing so, it is classified as not operational and the date of the last maneuver is used for the end of the operational phase. If it never performed an orbital maneuver a statistical based model is used to determine the operational status. From this date, if the satellite has not already left the protected region, it is propagated in order to predict the remaining time in that region. The eventual compliance of a satellite is a binary event (it either is or is not compliant), and can only truly be determined after the 25 years have passed. Therefore before that time, for an individual satellite the result can only be interpreted as a current best estimation.

3.1. Development cases

Two satellites were used during the development of the algorithm. This was done to immediately test and tune the settings and performance of the implemented methods. The two satellites chosen were Envisat and SARAL; some of their relevant properties are shown in Table 1.

These two satellites were chosen as the development cases for a combination of reasons. First, the satellites are both in SSO. Secondly, in order to develop the maneuver detection algorithm the date of the actual maneuvers has to be known. For both these satellites the International Laser Ranging Service (ILRS) publishes this data provided by the International DORIS Service (IDS). Finally, SARAL is much lighter than Envisat, allowing the algorithm to be developed for two different mass categories or better said: two different sensitivities to surface forces like aerodynamic drag.

3.2. Data sources

In this study use was made of different datasets provided by different sources. For orbital information use was made of Two Line Element (TLE) data provided by the United States Space Command (USSPACECOM) at https://www.space-track.org/ (Space-Track, 2021). For the maneuver detection algorithm validation use was made of maneuver data provided by the IDS. These data are published by the ILRS at https://ilrs.gsfc.nasa.gov/ (ILRS, 2021). Spacecraft information and descriptions were obtained from the Database and Information System Characterising Objects in Space (DISCOS). This database is maintained by ESA's Space Debris Office and provides information for all trackable unclassified objects in space at https://discosweb.esoc.esa.int/ (ESA, 2021) (Flohrer et al., 2013).

Table 1
Properties of the two development cases SARAL and Envisat. Obtained from ESA (2021) at https://discosweb.esoc.esa.int/.

Property	Satellite	
Name	SARAL	Envisat
SATCAT	39086	27386
Launch Year	2013	2002
Launch Mass [kg]	400	8200
Semi-Major Axis [km]	7163	7143
Inclination [deg]	98.5	98.1

4. Operational status determination

As the 25-year lifetime countdown only starts after the end of the active phase, the operational status of the satellite needs to be determined first.

4.1. Maneuver detection

The detection of potential maneuvers allows the determination of the operational status for spacecraft with orbital maneuver capabilities. The developed detection algorithm is primarily based on the TLE Time Series Analysis (TTSA) algorithm by Lemmens and Krag (2014) and has been taken a step further by some additions and modifications, such as a user-set global threshold acting as a sensitivity setting and a "grace period" during event detection preventing counting a single maneuver multiple times. For a more detailed mathematical description of the algorithm, the reader is referred to this particular reference. The procedure followed can be summarised in the following steps, which will be discussed more in-depth individually in the next sections:

1. Using a moving window, the semi-major axis is corrected for natural trends by a line fitted using repeated median regression with a Theil-Sen-Siegel estimator.
2. Based on the interquartile range (IQR) of this corrected series, a global lower and upper threshold is determined for the entire series.
3. In a moving window, a local lower and upper threshold is generated per epoch based on the IQR.
4. Using a Lomb-periodogram the presence of harmonics within each window is assessed. The amplitude of this is then added to the local threshold. The final threshold used for each epoch is the largest of the global and local threshold and a set minimum value.
5. Maneuvers are detected by checking the corrected series for events exceeding the thresholds.

4.1.1. Theil-sen-siegel estimator

The semi-major axis of a satellite in SSO will decrease over time in absence of any maneuvers. To separate this natural decay from maneuvers, a correction is made by fitting a line and subtracting this from the original data. Although the actual observed long-term effect of this

natural decay is not linear, it was found that over short timeframes it is sufficient to model it as one. This was done by making use of repeated median regression using the Theil-Sen Siegel Estimator by Siegel (1982) to determine the slope and intercept of the regression line $y = mx + b$, as shown in Eq. 1:

$$m = \underset{i}{median}\left(\underset{i\neq j}{median}\left\{\frac{y_j - y_i}{x_j - x_i}\right\}\right) \quad (1)$$

with intercept b determined by Eq. 2 (Siegel, 1982).

$$b = \underset{i}{median}\left(\underset{i\neq j}{median}\left\{\frac{x_j y_i - x_i y_j}{x_j - x_i}\right\}\right) \quad (2)$$

The effect of this repeated median variation can be seen in Fig. 5, where these two methods are shown together with a linear fit using a least squares estimator. Here random points were generated with a standard normal distribution variation along the line $y = x$ and outliers were added near the start and end of the series.

It can be seen that the Theil-Sen-Siegel method manages to best ignore the outliers and produce the most accurate slope and intercept and was therefore chosen as the estimator.

4.1.2. Threshold generation

The threshold generation is based on a user-set minimum and the IQR of both the global and local data points. It is therefore dynamic, allowing the thresholds to remain constantly low when the data is consistent and expand when the data is more noisy, as in the case of SATCAT 15427 in 2001 shown in Fig. 6. It was seen that this increase in noise is related to the solar cycle, this will be discussed more in Section 4.2.

4.1.3. Test cases

The maneuver data of two SSO satellites, Envisat and SARAL, were used for tuning and validation by comparison with their actual maneuver data as reported by the ILRS. The semi-major axis of Envisat in 2011 and 2012, together with detected and actual maneuvers is shown in Fig. 7.

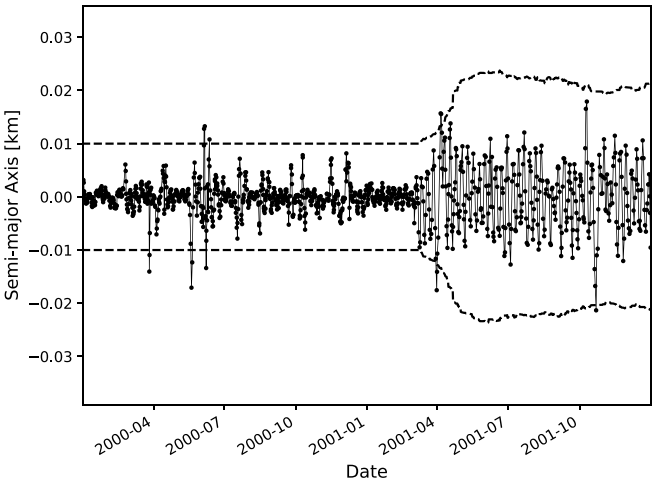

Fig. 6. Slope corrected time-series with generated thresholds for SATCAT 15427, using a user-set minimum of 10 m.

Multiple small-magnitude maneuvers can be observed, however after April 2012 these maneuvers suddenly stop, and will not reappear in the following years. This matches exactly with reported communication by ESA: "Just weeks after celebrating its tenth year in orbit, communication with the Envisat satellite was suddenly lost on 8 April. Following rigorous attempts to re-establish contact and the investigation of failure scenarios, the end of the mission is being declared" (ESA, 2012). It is exactly this moment, when the operational phase of the mission is over, that is of interest and it shows that for maneuvering satellites this can be determined by detecting these maneuvers.

It also shows that the algorithm manages to detect the date of the latest maneuver with sufficient accuracy. Secondly, when the orbital maneuvers are large, such as significant orbital lowering end-of-life maneuvers, the algorithm has no problem detecting them. However, when maneuvers

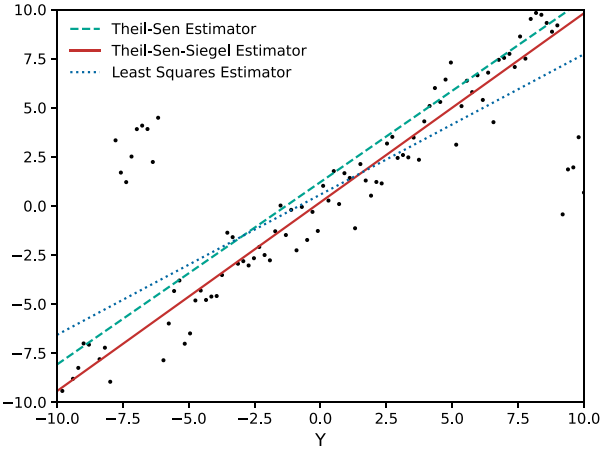

Fig. 5. Comparison of a line fitted using three different regression methods.

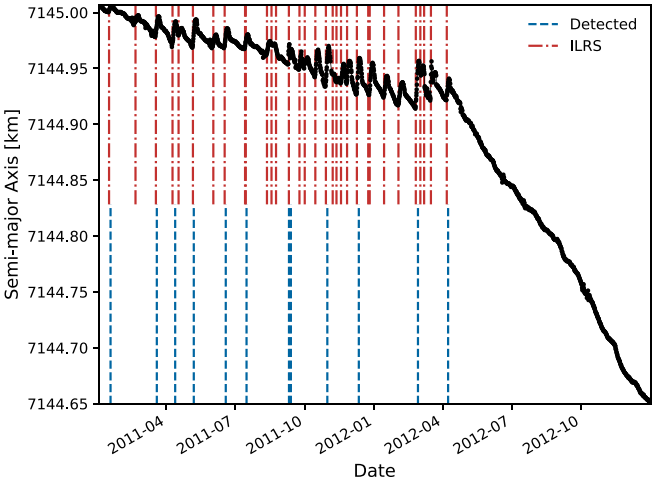

Fig. 7. Detected and actual maneuvers of Envisat as reported by the ILRS (ILRS, 2021).

are very small in magnitude, and especially when these are done in rapid succession, the algorithm struggles to detect all of them. This is because it is very difficult to distinguish this from being just noisy data. The ultimate purpose of this algorithm should also be kept in mind as it affects the required accuracy. It does not matter if the last detected maneuver date is a day, a week or even a month off; this will be discussed more in the next section.

4.1.4. Parameter tuning

The performance of the implemented algorithm was compared with the TLE Time Series Analysis (TTSA) and the TLE Consistency Check (TCC) algorithms by Lemmens and Krag (2014) and actual observed maneuvers. In their study 30 meteorological satellites operating in SSO were manually checked for existing maneuvers in 2011. The performance of the implemented algorithm was tested using three different sensitivity settings by changing the user-set global minimum threshold. The results can be found in Table 2; shown are only the satellites that were found to have actual maneuvers, or where one of the algorithms detected one.

The results can be categorised in maneuvering and non-maneuvering satellites, and have two types of errors: false positives, where a satellite is falsely concluded to have performed a maneuver, and false negatives, where the algorithm has falsely classified a satellite as not maneuvering. This classification is shown in Table 3.

The number of false positives decreases, and the number of false negatives increases as the limit is set to higher values. This is as expected, as this limit value can be interpreted as a sensitivity setting below which the data, and thus possible small maneuvers are ignored. Furthermore, it shows that the implemented algorithm performs better than the TCC and on-par with the TTSA algorithms. Finally, when going from 7.5 m to a limit of 10 m the first false negative appears. This means that using such a large limit creates the risk that a satellite that is actually maneuvering might not be detected as such.

Naturally one wants to keep both false positives and false negatives to a minimum. However, often one is vastly preferred over the other. In this case it is more unclear, as one could favour either one depending on the exact purpose. If one wants to detect every maneuver a satellite makes, it would make sense to make the algorithm very sensitive by making use of a low minimum threshold. This would come at the cost of detecting some maneuvers that have not actually happened.

For the purposes of this study the goal is to detect if a spacecraft has ever maneuvered and when it stopped doing so. Because there is such a long timeframe to analyse and detect possible maneuvers, the chance is increased that maneuvers are being detected somewhere. It is therefore beneficial to use a higher minimum threshold and accept the risk of missing some small maneuvers. It does not matter if one maneuver that was performed in a month is missed, if two others in the same month are detected.

4.2. Maneuver-based operational status

The maneuver detection algorithm was applied to all satellites in SSO. For each satellite the detected maneuver dates were recorded. An overview of the result of this can be found in Fig. 8. Shown here in the bottom part are the satellites that maneuvered in a given year, grouped by their launch year. Above that the solar flux intensity at 10.7 cm wavelength for the same period is given. Do note that spacecraft that perform orbit corrections with continuous low-thrust techniques will be harder to be identified by this algorithm as operational. However, the time domain covered by this study essentially runs from 1970 until 2020, and it is expected that the number of Sun-

Table 2
Detected maneuvers for different minimum threshold limits compared to literature and the actual performed maneuvers as manually identified.

SAT	Lemmens and Krag (2014)			Algorithm Performance		
CAT	Human	TCC	TTSA	5 m	7.5 m	10 m
15427	0	2	0	0	0	0
18123	1	1	1	3	3	3
19531	0	2	0	0	0	0
21263	1	1	1	1	1	1
21574	0	0	0	1	0	0
22739	0	4	0	2	1	0
23710	12	12	10	16	14	11
25682	16	15	11	26	28	25
25730	0	0	4	4	4	0
25994	8	8	7	17	18	17
26536	0	7	1	0	0	0
26620	3	3	3	6	3	5
27386	19	8	6	10	4	0
27421	6	7	7	9	10	9
27424	13	16	17	22	24	21

Table 3
Performance and errors classified by type of the maneuver detection algorithm for different minimum threshold limits compared to literature.

	Lemmens and Krag (2014)			Algorithm Performance		
	Human	TCC	TTSA	Limit = 5 m	Limit = 7.5 m	Limit = 10 m
Total Satellites	30	30	30	30	30	30
Maneuvering	9	13	11	12	11	9
Not Maneuvering	21	17	19	18	19	21
False Positives		4 (13.3%)	2 (6.7%)	3 (10.0%)	2 (6.7%)	0 (0.0%)
False Negatives		0 (0.0%)	0 (0.0%)	0 (0.0%)	0 (0.0%)	1 (3.3%)

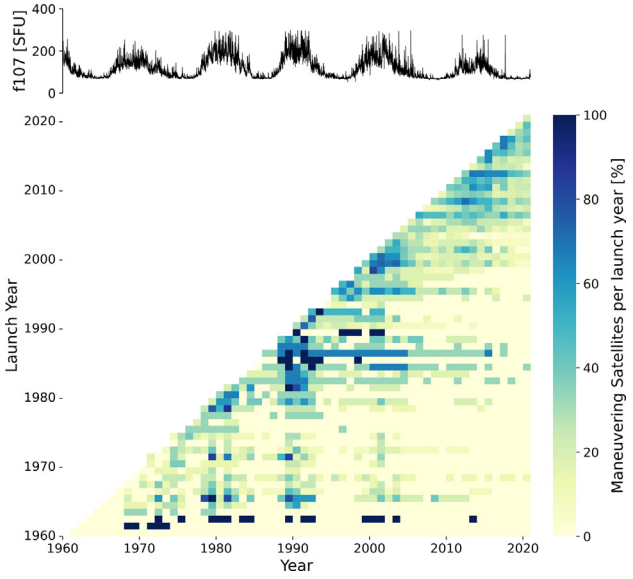

Fig. 8. Top: Solar flux intensity at 10.7 cm wavelength. Bottom: Maneuver matrix grouped by launch year colored by percentage of satellites that maneuvered in a given year.

synchronous spacecraft using such techniques is limited (still).

One would expect that the diagonal in this figure would show the highest percentage. As time goes by, this would be the horizontal direction in the figure, and as satellites stop functioning and maneuvering, one would expect to see a slow fade to the right, to eventually zero maneuvering satellites for a given launch year.

In general, this is also what is observed. However, Fig. 8 has some vertical bands where an increase in detected maneuvers appears. These bands correlate with the 11-year solar cycle. This can be explained by two possible causes. The first one is that the increase in drag prompts satellite operators to perform altitude increasing maneuvers. The second one is that this increase causes a change in the slope of the natural decay. Which is then incorrectly interpreted as the detection of a maneuver. These bands are more visible in the earlier cycles than in the recent ones. This has two reasons; first it can be seen that the past solar cycle has a distinct smaller maximum magnitude than the previous three. Secondly, it was observed that over time the data from the TLE have become more consistent and less noisy.

To prevent these false positives during these cycles, a filter was applied to the detected maneuvers. If a satellite has maneuvered in the past two years, this filter classifies the satellite as active. If at one time, the satellite has not performed a maneuver in the past two years, it is classified as inactive. Once inactive, the satellite can not be reclassified, even if a maneuver is detected for instance 10 years later.

4.3. Design lifetime model

The methods using the TLE data to detect orbital maneuvers, and therefore an operational status of a satellite, only work if such an orbital control system is present. Therefore for satellites without such a system, as is the case for many of the small satellites in LEO, an alternative method must be used. A possibility would be making use of reports published by the operators regarding the operational state of their satellites. However, as was stated earlier, these reports do not always exist and if they were to be used for compliance registration might not be accurate as well. One major indicator of operational status would be the existence of a radio signal from that satellite. There could be a system, either on the ground or in space, that would pick up all these signals and identify them. With this it might be possible to create an overview of the operational status for all spacecraft orbiting Earth with a high temporal resolution.

However, currently such a system does not exist, so for this group of satellites an alternative method was applied, based on statistical lifetime models. A variation of this was used by Morand et al. (2014), assigning different lifetimes to different types of satellites. The approach chosen was to make use of the design lifetime of the satellites. The information was obtained from literature (Maini and Agrawal, 2011) (Grimwood, 2020) and is displayed per mass category in Fig. 9.

It can be seen that satellites with a mass between 100 and 1000 kg show the most varying design lifetime with 3, 5, 8 and 15 years as the most popular choices. The number of satellites with a mass below 10 kg is relatively small in this design lifetime dataset, however cross-referencing the Nanosats Database (Kulu, 2021) shows similar results. Based on the distribution above, a single operational life-

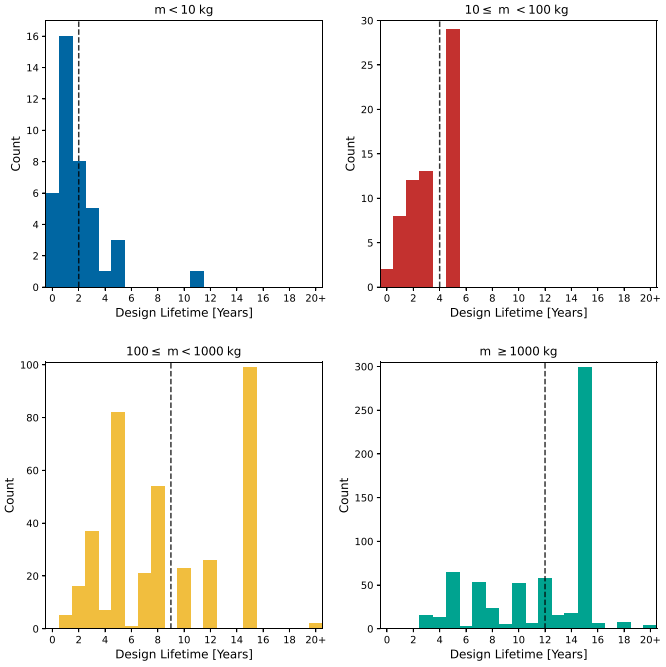

Fig. 9. Design lifetime of spacecraft for four different mass categories.

Table 4
Representative operational lifetime.

Mass Category	Operational Lifetime [Years]
m<10 kg	2
10⩽m<100 kg	4
100⩽m<1000 kg	9
m⩾1000 kg	12

time was chosen per mass category. This is shown in Table 4. This operational lifetime will be used for satellites without maneuver capabilities.

This does introduce some uncertainty in the results (a heavy spacecraft can be operational for 15 years for instance), but this concerns only a smaller part of the population.

4.4. Combined population

The results of the maneuver-based and non-maneuver-based operational status determination can be combined to generate a status overview for the entire population of satellites in SSO. The combined operational status can be classified in three different ways:

- *Operational*, if the satellite has maneuvered within the last two years or if it never maneuvered and is still within the design lifetime (Table 1).
- *Not Operational*, if the satellite has stopped maneuvering for the last two years or if it never maneuvered and is outside the design lifetime.
- *Unknown*, if the satellite has not maneuvered and was launched in the past two years.

The resulting combined operational status as a function of launch year can be found in Fig. 10. For obvious reasons, operational spacecraft are observed for the last 15 years only, non-operational objects are found anywhere in the time domain.

5. Orbital lifetime estimation

For the entire satellite population in SSO that was classified as not operational and observed to have decayed, the post-mission lifetime is straightforward to assess. For those that are not yet decayed, the remaining orbital lifetime was determined using the semi-analytical propagation method STELA, developed by CNES (Le Fèvre et al., 2012). The long-term mean evolution of the orbital elements is solved numerically and short-period effects have been removed. If the mean orbital parameters state at date t_n is represented by $E_n^{\bar{x}}$, then the state $E_{n+1}^{\bar{x}}$ at t_{n+1} is derived using the derivative $\frac{dE^{\bar{x}}}{dt}(t_n)$ which is calculated by (CNES, 2019):

$$\frac{dE^{\bar{x}}}{dt} = \frac{dE^{\bar{x}}_{Kepler}}{dt} + \frac{dE^{\bar{x}}_{Earth}}{dt} + \frac{dE^{\bar{x}}_{lunisolar}}{dt} + \frac{dE^{\bar{x}}_{drag}}{dt} + \frac{dE^{\bar{x}}_{SRP}}{dt} \tag{3}$$

where $\frac{dE^{\bar{x}}_{Kepler}}{dt}$ represents the movement due to the non-perturbed two-point gravitational force and $\frac{dE^{\bar{x}}_{Earth}}{dt}$ the perturbations due to Earth's irregular gravitational field. The term $\frac{dE^{\bar{x}}_{lunisolar}}{dt}$ represents third-body perturbations due to the gravitational forces of the Moon and the Sun. Finally, $\frac{dE^{\bar{x}}_{drag}}{dt}$ and $\frac{dE^{\bar{x}}_{SRP}}{dt}$ represent perturbations due to atmospheric drag and solar radiation pressure respectively. This is solved by a numerical integrator based on a fixed-timestep sixth-order Runga-Kutta method.

The osculating parameters are then computed in the integration intervals according to:

$$E_n^{osc} = E_n^{\bar{x}} + E_n^{shortperiod} \tag{4}$$

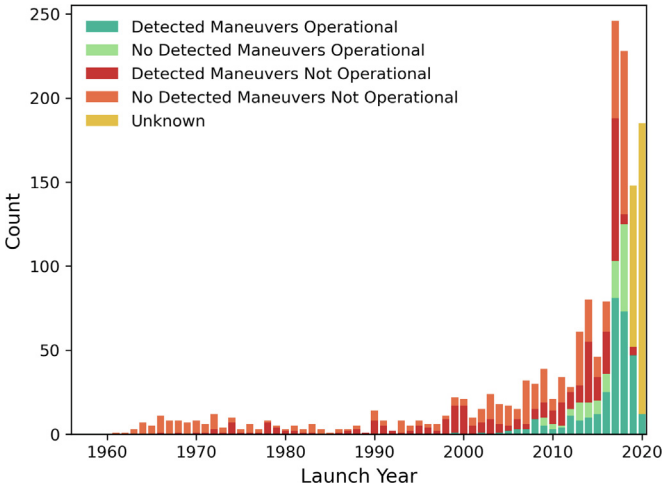

Fig. 10. Operational status of all satellites in SSO on January 1, 2021.

where $E_n^{shortperiod}$ is solved analytically and includes short-period effects from irregularities of the gravity field, Solar and Lunar gravity, atmospheric drag and Solar radiation pressure.

This resulted in a total lifetime after the operational phase in years, for each satellite in SSO.

6. Compliance

With this total remaining lifetime known, the compliance of each satellite can now be classified as:

- *Compliant*, if the remaining orbital lifetime after the operational phase is less than 25 years.
- *Not Compliant*, if the remaining orbital lifetime after the operational phase is more than 25 years.

This was determined for all satellites for which no maneuvers were detected, and are therefore assumed to be in their ballistic phase. This also includes the satellites that have already decayed. For these satellites of course the exact re-entry date is known and no orbital lifetime estimation was needed. An overview of the total satellites analysed, their operational status and orbital control capabilities is given in Table 5. The following results will therefore not include the satellites that have maneuvered within the past two years, as they would have the potential to lower or raise their orbits. Also not included are the satellites that were launched within the past two years as the operational status could not yet be determined for those. Remaining are the 980 not operational, of which 110 have already decayed, and the 126 operational satellites without orbital control capabilities. As for the 278 satellites that were classified here as "status unknown", they were not included in any of the subsequent evaluations. Also, it is recommended to (try to) obtain information on their status by contacting their operators and/or inspecting public information available on internet or in any other sources (although this is recognized to be quite challenging).

The compliance was determined for these 1106 satellites and is shown, as a percentage of satellites launched in a given year, in Fig. 11. In this figure an increasing compliance trend can be observed starting around 2010 when compliance was 20 to 40%, to around 95% compliance in 2017 and 2018.

Table 5
Overview of the number of satellites in SSO and their operational status.

Status	Satellites
Not Operational	980
with orbital control capability	332
without orbital control capability	648
Operational	358
with orbital control capability	232
without orbital control capability	126
Unknown	278
Total	1616

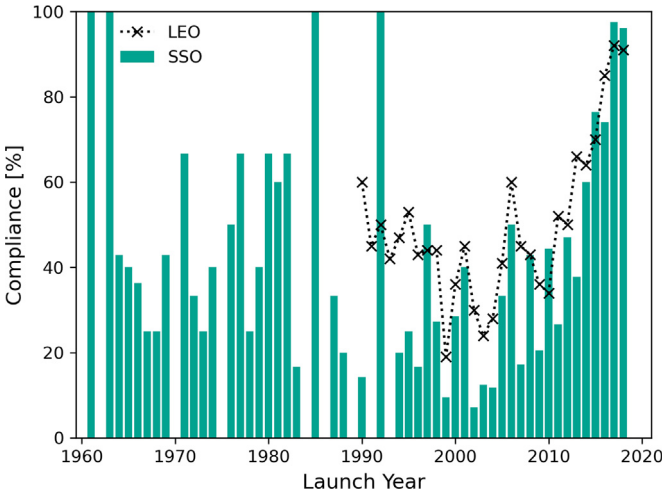

Fig. 11. Compliance of satellites in SSO with the 25-year lifetime rule. The dotted line shows the results for the entire LEO population as derived by ESA (ESA Space Debris Office, 2020).

When comparing SSO to the results obtained for the entire population of LEO satellites by ESA (ESA Space Debris Office, 2020), it can be seen that the SSO satellites follow the same trend but have generally been underperforming a bit in the past. A study done by CNES found for LEO satellites launched between 2000 and 2013 a compliance rate of 59%, but observed no meaningful trend in global compliancy with the 25-year lifetime rule (Morand et al., 2014). Comparing this to the results found in this study for this period, a lower compliance was observed here, between 15 and 50%. However, just like Morand et al. (2014) no trends were visible in this timeframe, with a positive trend starting later, only from 2014 onwards.

In Geosynchronous orbit (GSO) however, it can be seen that the positive compliance rate trend already started much earlier, starting in the late 1970s compared to mid 2010s for LEO (Pallas and Noomen, 2018). The GSO satellites reached a compliance rate of 70% already in the early 90's and are expected to have an almost 100% compliance rate since 2010, although their long mission duration introduces an inherit large lag in available data (ESA Space Debris Office, 2018). Furthermore, since the natural decay for a satellite in GSO is so small, they have to rely exclusively on end-of-life maneuvers to remove themselves from the protected region. This capability of maneuvering of every satellite, combined with the used slotting system in GSO, may be the reason of this multi-decade lead in compliance. Weeden and Shortt (2008) concluded that such a slotting system could also provide benefits in long-term operating safety and sustainability for SSO, but due to the inherit mechanics in this regime this is much more complicated than the GSO slots.

To determine what is driving the recent increase in compliance in SSO it is useful to group the satellites in different mass categories. The overall compliance per mass category is displayed in Table 6. While a large fraction of the

Table 6
Compliance rate of different mass categories.

Mass Category	Compliant [%]	Not Compliant [%]
m < 10 kg	86.4	13.6
10 ⩽m < 100 kg	36.2	63.8
100 ⩽m < 1000 kg	33.2	66.8
m ⩾1000 kg	32.8	67.2

smallest satellites is compliant, a large difference between this group and the rest of the mass categories can be observed.

This might at first be counter-intuitive: after all the operational phase of a smaller spacecraft is often significantly lower than that of a spacecraft with a higher mass, allowing less time for a satellite to decay. However, the most dominant reason that smaller satellites are more often compliant is due to the orbits they are initially launched in. This is shown in Fig. 12, where a distribution of the altitude of the initial orbit is shown for each of the four mass categories. Clearly, the smaller spacecraft are launched in lower orbits, and assuming that the (average) ballistic coefficients do not vary that much over the entire population, they are prone to smaller residual lifetimes.

This relationship, between initial orbit and eventual compliance, is even more visible when dividing the mass categories in their respective compliance groups as done in Fig. 13.

This is as expected, after all a lower initial altitude will expedite the natural orbital decay. To investigate the behaviour of satellite operators further, the compliance rate is grouped by their orbital control capability (OCC). This was determined by the presence of any detected maneuver for each satellite.

In Table 7 it can be seen that there is no large difference and even a slightly higher compliance for satellites without OCC. Once again, this can be explained by the fact that the smaller satellites often do not have this capability, and as was seen, these satellites are launched in lower orbits and

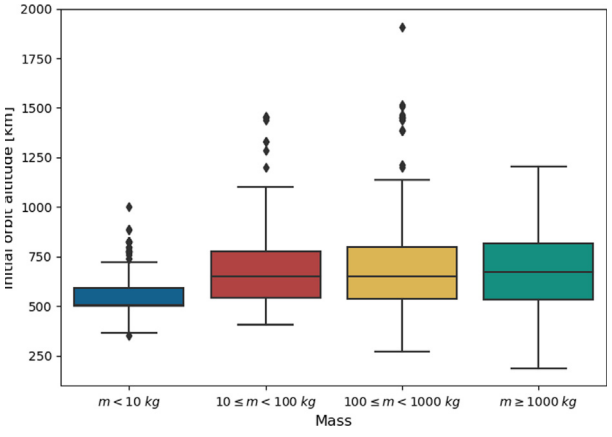

Fig. 12. Initial orbit altitude distribution per mass category.

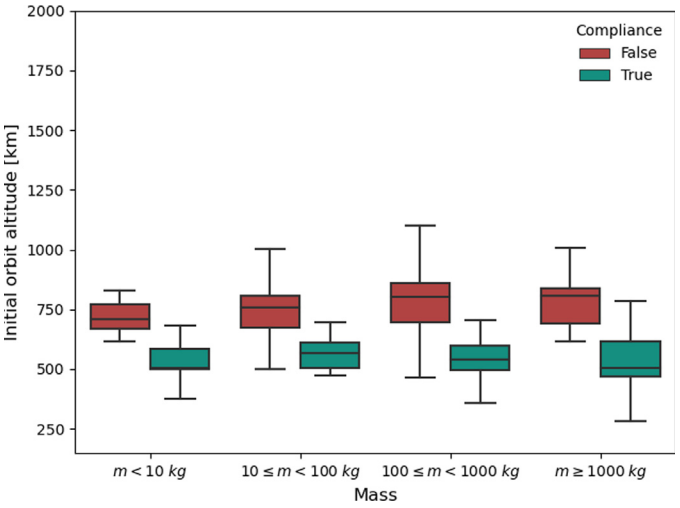

Fig. 13. Initial orbit altitude distribution per mass category and compliance. Altitude here is determined by the semi-major axis minus the mean equatorial radius of the Earth.

Table 7
Compliance rate for satellites with orbital control capabilities and those without.

Capability	Compliant [%]	Not Compliant [%]
Orbit Control	55.7	44.3
No Orbit Control	60.3	39.7

are therefore more often naturally compliant. This indicates that in the past the capability of orbital maneuvers has been minimally used for accelerated de-orbiting.

6.1. Time limit adjustment

With the large number of spacecraft launched every year one might want to make the regulations more strict. The effects of reducing this 25-year time limit can be seen in

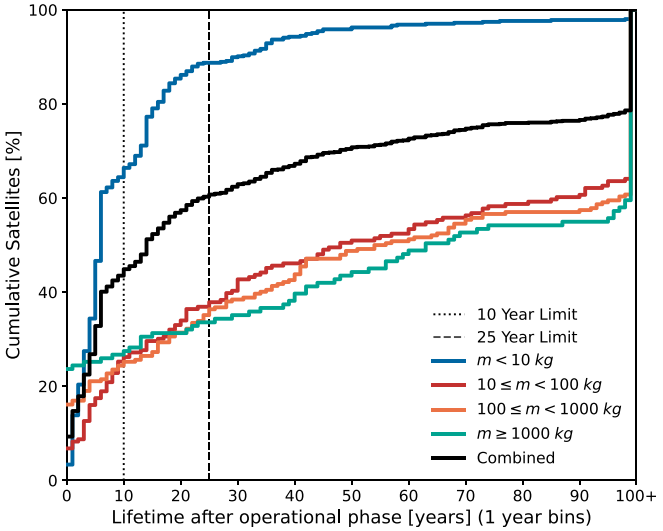

Fig. 14. Cumulative distribution of remaining orbital lifetime after the operational phase. The final bin includes lifetimes higher than 100 years.

Fig. 14. Of course it should be noted that recent launches should have been designed with the aim of 25 years, and older satellites even without any regulations at all. However, it does give insight on what these compliance rates currently would be.

The key takeaway here is that the smallest satellite group achieves a fairly high compliance rate even with stricter maximum allowed lifetimes: achieving a compliance rate of more than 60% with a maximum lifetime of 10 years. This seems to be an interesting possible change in current requirements.

7. Conclusions

It was seen that the number of objects launched to LEO has seen a huge increase in the past years, mainly due to commercial launches. The growing launches by smaller companies or agencies, made possible due to the increasing accessibility to space, together with the upcoming satellite constellations, will lead to the number of satellites in the near future to increase tremendously. Very noticeable were the different clusters of satellites in LEO, when grouped by altitude and inclination. Here especially SSO was seen to be a very popular choice, with the large increase in satellites launched to SSO primarily driven by satellites with a mass below 10 kg.

The compliance with the guidelines has been quite poor in the past, but has been improving significantly in recent years starting from 2014. Furthermore, there is a large difference between the different mass categories. Whereas 86% of the satellites with a mass less than 10 kg are compliant, the other mass categories only reach a compliance of around 35%. It was also observed that there was no large difference between the compliance of satellites with orbital control capabilities compared to those without. It was shown that compliance is mostly a result of choosing an orbit with a sufficiently low altitude to have a sufficient natural decay, and less of operators choosing to perform altitude-lowering maneuvers at the end of the operational phase to achieve compliance.

A potential follow-up of this study would best be aimed at the issue of satellites with an ”unknown” status: would it be possible to assess these by contacting individual operators or publicly available data sources? These sources could also be used to verify the operational status findings using orbital behaviour. In addition, in view of the possibility to use continuous low-thrust for orbit maintenance, also in SSO, it is worthwhile to focus some attention to the orbital behaviour of such satellites and to investigate whether the algorithms applied here are able to recognize their status properly. Finally, a further development of the techniques to eliminate as many false positives and false negatives as possible is also welcomed.

The large increase in the number of launches in recent years does also trigger the question if current guidelines are sufficient to protect the long-term sustainable use of space. Looking specifically at the relative popularity of SSO, it may need re-evaluation to sustain future spaceflight operations in these valuable orbits.

Declaration of Competing Interest

The authors declare that they have no known competing financial interests or personal relationships that could have appeared to influence the work reported in this paper.

References

Anselmo, L., Portelli, C., Tremayne-Smith, R., Alby, F., Baccini, H., Bonnal, C., Alwes, D., Flury, W., Jehn, R., Klinkrad, H., 2004. European code of conduct for space debris mitigation. United Nations Office for Outer Space Affairs. Issue 1.0.

Bonnal, C., 2016. A brief historical overview of space debris mitigation rules. Presentation at Clean Space Industrial Days. ESTEC, Noordwijk The Netherlands.

Bonnal, C. (2019). Space debris mitigation & remediation: a general update. In JAXA Special Publication: Proceedings of the 8th Space Debris Workshop (pp. 157–171). Japan Aerospace Exploration Agency volume JAXA-SP-18-011.

Brooks, D., Bess, T., Gibson, G., 1974. Predicting the probability that Earth-orbiting spacecraft will collide with man-made objects in space. In: 25th International Astronautical Congress A74–34.

CNES, 2019. STELA User Manual Version 3.3. Technical Report CNES.

ESA, 2012. Esa declares end of mission for envisat. URL: http://www.esa.int/Applications/Observing_the_Earth/Envisat/ESA_declares_end_of_mission_for_Envisat accessed on: 2020-10-12.

ESA, 2021. Database and information system characterising objects in space. URL: https://discosweb.esoc.esa.int/ accessed on: 2021-12-12.

ESA Space Debris Office, 2018. Classification of geosynchronous objects. Technical Report GEN-DB-LOG-00211-OPS-GR.

ESA Space Debris Office, 2020. ESA’s Annual Space Environment Report. Technical Report GEN-DB-LOG-00288-OPS-SD.

Flohrer, T., Lemmens, S., Virgili, B.B., Krag, H., Klinkrad, H., Parrilla, E., Sanchez, N., Oliveira, J., Pina, F., 2013. Discos-current status and future developments. In: Proceedings of the 6th European Conference on Space Debris, vol. 723. pp. 38–44.

Grimwood, T., 2020. The union of concerned scientists satellite database. URL: https://www.ucsusa.org/resources/satellite-database accessed on: 2021-01-01.

IADC Steering Group and Working Group 4, 2002. Space debris mitigation guidelines. Inter-Agency Space Debris Coordination Committee, (IADC-02-01).

ILRS, 2021. Satellite maneuvers. URL: https://ilrs.gsfc.nasa.gov/data_and_products/predictions/maneuver.html accessed on: 2021-01-01.

Johnson, N., 2007. Developments in space debris mitigation policy and practices. Proc. Inst. Mech. Eng., Part G: J. Aerospace Eng. 221 (6), 907–909.

Kato, A., Lazare, B., Oltrogge, D., Stokes, H., 2013. Standardization by ISO to ensure the sustainability of space activities. In: 6th European Conference on Space Debris, vol. 723, p. 119.

Kessler, D.J., Cour-Palais, B.G., 1978. Collision frequency of artificial satellites: The creation of a debris belt. J. Geophys. Res.: Space Phys. 83 (A6), 2637–2646.

Kulu, E., 2021. Nanosats database. URL: https://www.nanosats.eu/ accessed on: 2021-01-01.

Le Fèvre, C., Fraysse, H., Morand, V., Deleflie, F., Wailliez, S., Lamy, A., Martin, T., Perot, E., 2012. Long term orbit propagation techniques developed in the frame of the french space act. In: Ouwehand, L. (Ed.), Proceedings of the 5th IAASS conference - A Safer Space for Safer World. ESA Communications, Noordwijk, the Netherlands, p. 89.

Lemmens, S., Krag, H., 2014. Two-line-elements-based maneuver detection methods for satellites in low Earth orbit. J. Guidance, Control, Dyn. 37 (3), 860–868.

de Luca, L., Bernelli, F., Maggi, F., Tadini, P., Pardini, C., Anselmo, L., Grassi, M., Pavarin, D., Francesconi, A., Branz, F., Chiesa, S., Viola, N., Bonnal, C., Trushlyakov, V., Belokonov, I., 2013. Active space debris removal by a hybrid propulsion module. Acta Astronaut. 91, 20–33.

Maini, A.K., Agrawal, V., 2011. Satellite Technology: Principles and Applications. John Wiley & Sons, Hoboken, NJ, USA.

Morand, V., Dolado-Perez, J.-C., Philippe, T., Handschuh, D.-A., 2014. Mitigation rules compliance in low Earth orbit. J. Space Saf. Eng. 1 (2), 84–92.

Pallas, P., Noomen, R., 2018. GEO satellites end-of-life disposal - compliance status. In: 69th International Astronautical Congress. International Astronautical Federation (IAF). AC-18.A6.4.7.

Siegel, A.F., 1982. Robust regression using repeated medians. Biometrika 69 (1), 242–244.

Space-Track, 2021. The source for space surveillance data. URL: https://www.space-track.org/ accessed on: 2021-12-12.

Weeden, B., Shortt, K., 2008. Development of an architecture of sun-synchronous orbital slots to minimize conjunctions. In: Advanced Maui Optical and Space Surveillance Technologies Conference, p. E72.